Available online at www.sciencedirect.com
SCIENCE DIRECT
Polymer 47 (2006) 2741–2749
polymer
www.elsevier.com/locate/polymer

Matrix physical structure effect on the electro-optic characteristics of thiol–ene based H-PDLC films

Askim F. Senyurt [a], Garfield Warren [b], Joe B. Whitehead Jr [b], Charles E. Hoyle [a,*]

[a] Department of Polymer Science and Engineering, University of Southern Mississippi, Hattiesburg, MS 39406, USA
[b] Department of Physics and Astronomy, University of Southern Mississippi, Hattiesburg, MS 39406, USA

Received 25 October 2005; received in revised form 17 February 2006; accepted 17 February 2006
Available online 14 March 2006

Abstract

The physical and mechanical properties of several thiol–ene based polymers and their mixtures with the liquid crystal, E7, were characterized to probe their relationship with the liquid crystal film electro-optic performance properties. Kinetic data suggests that high conversion is achieved for each thiol–ene combination. Pre-polymerization phase diagrams indicate that each thiol–ene/E7 mixture phase separates well below room temperature, and thus prior to polymerization at room temperature all are in a single phase. Holographic polymer dispersed liquid crystals (HPDLC) were fabricated for several thiol–ene and E7 mixtures, and electro-optical parameters characterized to probe the relationship between the thiol–ene network properties and the electro-optic performance of the HPDLCs. The photocured matrices exhibited glass transitions and tan δ peak maxima that ranged from temperatures below 0 °C to well above room temperature. There is a clear correlation between the physical nature of the matrix and the electro-optic switching parameters with H-PDLC films fabricated from trithiol-pentaerythritol triallylether, all of which exhibit glass transition temperatures below 0 °C, having the fastest switching times and lowest switching voltages at room temperature. Also, in each case higher liquid crystalline concentration resulted in lower switching voltages.

Keywords: H-PDLC; PDLC; Phase separation

1. Introduction

Holographic polymer dispersed liquid crystals (H-PDLCs) are a relatively recent version of the extensively studied polymer dispersed liquid crystals (PDLC) [1–45]. H-PDLCs, unlike conventional PDLCs, contain alternating planes of polymer matrix and liquid crystal (LC) droplets. Conventional PDLCs are fabricated by the exposure of a photo-reactive monomer/LC mixture sandwiched between two conductive glass plates to a broad-band UV light source. The conversion of monomer to polymer destabilizes the initially homogeneous mixture and results in a phase separated random dispersion of micron-sized liquid crystal droplets surrounded by solid polymer. In the case of H-PDLCs, the reactive monomer/LC mixtures are holographically illuminated using laser light. The phase separated morphology for H-PDLCs consist of alternating planes of sub-micron liquid crystal droplets and solid polymer [1–45].

H-PDLCs diffract visible light due to the refractive index modulation that results from the alternating planes of sub-micron liquid crystal droplets and polymer planes. H-PDLCs may be fabricated as transmission or reflection grating and are switchable when subjected to an external electric field. These features of H-PDLCs make them candidates for electro-optic applications such as displays [39–41], diffractive optics [42], fiber optics [43], remote sensing [44] and many others [45].

Due to the variety of applications, it is crucial to be able to manipulate and improve the electro-optical performance of H-PDLC films such as switching speeds and voltages, diffraction efficiency, and contrast. Bunning et al. [27–38,41,42] and Crawford et al. [1–12,40,44] published several papers dealing with morphological development and the electro-optic properties of H-PDLC films. They evaluated the effect of exposure time and laser beam intensity [15,17,22,32,37], concentration of LC and polymer matrix [1,31,37], and temperature [11,17,37] on the H-PDLC electro-optic switching properties. They concluded that electro-optic properties are related to such parameters as the phase separated morphology.

* Corresponding author. Address: Department of Polymer Science, University of Southern Mississippi, P.O. Box 10076, Hattiesburg, MS 39406, USA. Tel.: +1 601 266 4873; fax: +1 601 266 5504.
E-mail address: charles.hoyle@usm.edu (C.E. Hoyle).

0032-3861/$ - see front matter © 2006 Elsevier Ltd. All rights reserved.
doi:10.1016/j.polymer.2006.02.049

Bunning et al. [27] published a recent review article that summarizes the relevant H-PDLC literature.

The majority of the H-PDLC literature is focused on photocurable acrylate systems [1–17,21,22,24,26,29,31–33,35,36]. Unfortunately, there are distinct disadvantages of acrylate systems; high shrinkage, low conversion, early gel point, oxygen inhibition, and formation of a non-uniform crosslinked matrix due to early micro-gelation. These parameters can have a distinct effect on the operational stability of the grating spacing and the electro-optic properties of the films [5,21,22,28,30,36,38].

Photopolymerizable thiol–ene based resins are alternatives that overcome some of the problems associated with acrylate based H-PDLCs and have received recent attention [28,30,48]. Thiol–ene free-radical polymerization processes have been well-known for about fifty years. Progress in this area is well documented by reports from Jacobine et al. [46], Bowman and Cramer et al. [47] and Hoyle et al. [48]. The free-radical chain reaction between a thiol and an ene proceeds by a step-growth process, a free radical addition followed by a chain-transfer reaction. H-PDLCs [18–20,28,30] and conventional PDLCs fabricated from thiol–ene systems exhibit improvements in uniformity of LC droplet size and shape, switching speeds, contrast ratios and high transmission in the on state [28,30]. All of the PDLC and H-PDLC reports in the literature dealing with thiol–ene based resins have centered on a single system, Norland 65, comprised of a tetrafunctional ene and a trifunctional thiol. Norland 65, when combined with the E7 liquid crystal mixture, gives rise to PDLCs and H-PDLCs with good switching and optical properties, due in great part to the proper balance of the birefringent refractive index properties of the E7 liquid crystal and the thiol–ene matrix. The tetrafunctional ene in Norland 65 has two urethane groups per molecule and thus it is effective in inducing phase separation due to the mismatch in solubility parameters between the urethane groups and the cyanobiphenyl LC components. Moreover, it is well known that urethane groups form hydrogen bonds, thus adding another dimension to network buildup and phase separation between the thiol–ene network and LC components. Urethane groups associate via hydrogen bonding, with the extent of hydrogen bonding depending upon the urethane concentration and the equilibrium constant between the associated and unassociated urethane groups. Introduction of a diluting component, i.e. the liquid crystal, results in a system in which the extent of hydrogen bonded versus free urethane groups changes as a complicated function of the diluting component concentration. Hydrogen bonding is present in both the pre-cured mixture and the final network, although it is assuredly different in each. This can certainly present a profound problem when trying to interpret the basic pre-polymerization phase diagram and its relationship to polymerization kinetics and film formation. Also, hydrogen bonding will also have a distinct effect on the nature of the cured matrix properties and the resulting electro-optic responses. The amount of liquid crystals dissolved in the continuous matrix will affect the hydrogen bonding thus making it more difficult to correlate polymer physical properties and electro-optic response.

As mentioned, all thiol–ene H-PDLCs to date have been fabricated from Norland 65, which we have recently found to have a fairly high glass transition temperature above room temperature. In order to be in a better position to design new matrices for H-PDLCs involving thiol–enes, we wanted to answer a basic question: 'what role does the physical state of the matrix at the temperature which the electro-optic measurements are made have on the critical switching parameters of voltage and time'. To answer this question, it is necessary to evaluate electro-optic properties at a single temperature for several H-PDLC matrices in different physical states (rubber, glass) at that temperature. It is important to do this in the absence of the influence of hydrogen bonding, which would complicate the interpretation of the results. Accordingly, three thiol–ene systems in which a common trifunctional thiol is photopolymerized with three distinct enes that do not contain urethane groups were evaluated with respect to their physical/mechanical properties in the presence of varying concentrations of liquid crystal. The three cured thiol–ene systems indeed have different physical states at room temperature, and therefore, the electro-optic properties should be reflective of the physical/mechanical configuration of the network, thereby allowing the basic relationship between physical state and switching parameters to be determined. Thermal and dynamic mechanical analysis results of cured networks with a wide variation in the liquid crystal concentration were correlated with the H-PDLC electro-optic performance. A single liquid crystal mixture, E7, was chosen for use in each thiol–ene system. The diffraction properties, which depend upon on the refractive index of the matrix and the liquid crystal mixture among other factors, were therefore not optimized since this would have required selecting a different liquid crystal mixture for each matrix, thus prohibiting a valid comparison of physical state and electro-optic switching properties. By keeping the liquid crystal type constant, a direct comparison between matrix physical state and switching voltage and times was thus obtained.

2. Experimental

2.1. Materials

Trimethylolpropane tris(3-mercaptopropionate), pentaerythritol triallyl ether, triallyltriazine trione, and triallyloxytriazine were obtained from Aldrich Chemical Company. The nematic liquid crystal mixture, E7, was obtained from EM industries. The initiator 2,2-dimethoxy 2-phenyl acetophenone (DMPA) was obtained from Ciba Specialty Chemicals. All chemicals were used as received without further purification.

2.2. Methods

Pre-polymerization monomer/LC mixtures were examined using temperature controlled optical microscopy to identify the phase separation temperature, and thus establish thermal phase

diagrams. The sample mixtures were sandwiched between a microscope slide and a cover slip using 10 μm spacers. Phase separation temperatures were determined by using a Linkham Scientific LTS350 hot stage and controller with a heating/cooling rate of 10 °C/min.

A thin-film calorimeter (TFC) was used to monitor polymerization exotherms of mixtures of the trifunctional thiol with pentaerythritol triallyl ether, triallyltriazine trione and triallyloxy triazine. A TFC measures the heat flow and converts it into an electrical signal with a thin-film heat flux sensor. Advantages of TFC compared to conventional photo differential scanning calorimetry (photo-DSC) include a simple experimental setup for polymerization exotherm measurements of thin films, the ability to easily control the sample thickness, and the ability to measure exotherms for volatile monomers. Applications of TFCs are well documented elsewhere [49–52]. Samples were prepared by mixing trithiol with each one of the enes based on equal molar functional group concentration. The amount of UV initiator, DMPA, was 1 wt% of the total thiol–ene mixture. Samples of 5–10 μm thickness were placed on the heat flux sensor with a glass cover slide. UV light intensity at the sample position was measured by a calibrated radiometer (International Light IL-1400).

The conversion as a function of irradiation time was recorded on a modified Bruker 88 spectrometer with a 200 W high pressure mercury–xenon lamp source. In the real-time infrared measurements, polymerization of 5 μm films was initiated with a light intensity of 1.4 mW/cm^2 at 365 nm. The thiol group conversion was monitored by measuring the peak height of the 2570 cm^{-1} band, while the peak at a 1645 cm^{-1} was used for ene double bond conversion calculations in each case.

The PDLC samples used for mechanical and thermal analysis were cured with a UV Fusion line EPIQ 6000 (D bulb, 3.15 W/cm^2) at a line speed of 10 ft/min. Dynamic mechanical analysis of the cured films was performed using a TA Q800 by heating the samples from −50 to 100 °C at a rate of 3 °C/min and at frequency of 1 Hz in air. DMA was conducted using the shear sandwich mode for 10×10 mm^2 size samples with thicknesses of 150–200 μm. A TA Q1000 differential scanning calorimetry (DSC) was used to monitor thermal transitions by heating/cooling 5–10 mg samples from −50 to 100 °C at a rate of 10 °C/min under a nitrogen purge.

In addition, H-PDLC transmission gratings were fabricated with the same thiol–ene and E7 combinations for which polymerization induced phase separation occurred. $1''\times1''$ Cells fabricated from ITO coated glass were capillary filled and holographically illuminated with the interference pattern of the split and recombined laser light from a Spectra-Physics Beamlok argon ion laser with output at 364 nm. The optical setup was arranged to fabricate transmission gratings with an 18° angle between the reference and object beams. H-PLDC gratings were post-cured for 20 min using flood exposure from a broad-band UV light source.

Voltage-dependent laser light transmission measurements were used to probe the electro-optic properties, and thus the spatial and compositional aspects of the phase-separated morphology of the HPDLCs. The voltage dependent intensities of the zero and first order diffractions of p-polarized light at $\lambda=$ 633 nm were measured upon the application of an applied voltage. Each sample was first subjected to a 1 kHz ramped waveform of 500 ms in duration to determine the voltage required to reach 90% transmission, V_{90}. The sample was then subjected to a 1 kHz sine wave pulse of 50 ms in duration with constant amplitude equal to V_{90}. The data was analyzed to compute the voltage dependent intensities of the zero and first order diffractions and ultimately the voltage dependent diffraction efficiency and switching time.

Scanning electron microscopy (SEM) was used to probe the spatial aspect of the phase-separated morphology. SEM images were obtained using a Quanta 200 SEM in the high voltage mode. The H-PDLC samples were freeze fractured, soaked in hexane for 48 h, and placed under vacuum for 24 h to remove the liquid crystals from the exposed surface [53]. The freeze-fractured samples were mounted on the SEM sample holders and sputter coated with gold using a Polaron E5100 sputter coater before imaging.

3. Results and discussion

In this report, we present results of a systematic investigation of the material properties of several different thiol–ene based polymer matrices with liquid crystal mixture, E7, present. The question of how structural features of the monomer components affect the properties of the phase separated networks is addressed. Specifically, we carried out a study of basic crosslinked networks formed by reacting a single trifunctional thiol with three trifunctional ene monomers with very different structural features; pentaerythritol triallyl ether, triallyltriazine trione, and triallyloxytriazine (see Diagram 1 for structures). To set the stage for electro-optical measurements, we evaluated both the inherent properties of the pre-polymerization mixtures and the resultant matrices produced when exposed to incoherent UV light in the presence of the liquid crystal E7. Different weight percentages of E7 (components, structures and concentrations are given in Diagram 2) were added to the monomer mixture with the aim of monitoring the phase changes of the pre-polymerization mixtures by optical microscopy. Then, samples for physical and mechanical property evaluation were prepared by flood exposure with a medium pressure mercury lamp. Glass transitions were determined by differential scanning calorimetry (DSC) and dynamic mechanical analysis (DMA) to provide a basic analysis of the physical and mechanical properties of the base films. Although, these films evaluated by DSC and DMA are not identical to the final H-PDLC films prepared by exposure to the laser, they do provide a basic framework for characterizing the mechanical and physical properties of thiol–ene films that result from the trithiol with each of the three enes. Finally, the phase-separated morphology of the H-PDLC gratings were probed using scanning electron microscopy (SEM), and electro-optic properties were measured.

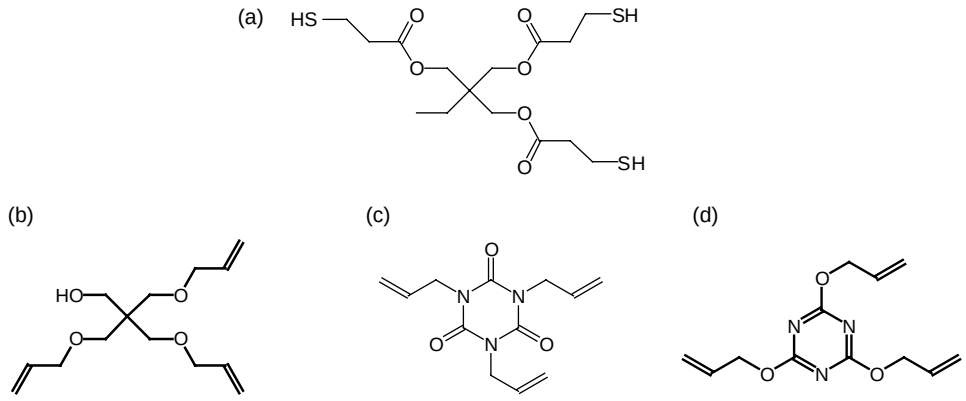

Diagram 1. Chemical structures of (a) trimethylolpropane tris(3-mercaptopropionate), (b) pentaerythritol triallyl ether, (c) triallyltriazine trione, and (d) triallyloxy triazine.

3.1. Phase diagrams of pre-polymerization mixtures

Phase diagrams of pre-polymerization mixtures of LC with reactive monomers show thermally induced phase separation depending on the LC content and temperature [54]. Such pre-polymerization phase diagrams can provide critical information about the thermodynamic stability of the starting LC/monomer mixture as a function of temperature and composition. Having a complete description of the initial phase behavior is important in understanding the phase separation of LC during polymerization and the final morphology of the H-PDLC film [54]. Consequently, in the present investigation, phase diagrams of LC/monomer mixture were established by varying the LC concentration from 0 to 80 wt% and the temperature from −30 to 60 °C as shown in Fig. 1. All samples with less than 30 wt% LC were miscible at all temperatures over the range measured, and hence only data for mixtures with 30–80 wt% LC are shown in Fig. 1. It is clear from the results in Fig. 1 that the solubility behavior of each of the three monomer/LC mixtures is characterized by a phase diagram such that for each composition there is a temperature above which the mixture is a single phase. According to Fig. 1, samples at room temperature with LC concentrations ranging from 30 to 50 wt% are single phase, well above temperatures where two phases exist. Thus, samples in this range will be single phase prior to initiating polymerization, provided that the polymerization is conducted at room temperature (∼24 °C).

3.2. Polymerization kinetics of thiol–enes

Polymerization exotherms of each of the thiol–ene mixtures in the absence of added LC were next obtained using both a thin-film calorimeter (TFC) and a real time infrared spectroscopy (RTIR) to provide kinetic analysis. The polymerization exotherms in Fig. 2 and RTIR based percent conversion versus time plots in Fig. 3 show that all three of the pure (i.e. without adding LC) thiol–ene mixtures polymerize efficiently within several seconds to high conversions. We have recently shown that the TFC can be used to accurately record the exotherms of thin films, while the traditional photo-DSC cannot be used to measure the polymerization exotherms of thin films or to measure exotherms of samples with competitively absorbing materials (pigments, inert fillers, etc.) [49–52]. Accordingly, we extended the TFC measurements in Fig. 2 for the pure thiol–ene systems to record the exotherms of the same thiol–enes with increasing concentrations of added E7 at a thickness of 10 μm; this is essentially identical to the configuration that will be used to produce the H-PDLCs to be discussed in subsequent sections, except that in this case a medium pressure lamp is used to induce the polymerization process. In Fig. 4, TFC exotherm results for the trithiol/triallyltriazine trione mixture with 0–50 wt% E7 clearly show that addition of E7 systematically reduces the polymerization rate. The relative area under the curve decreases in the ratio of 1.0:0.96: 0.62:0.65: 0.47:0.44 as the thiol–ene functional group concentration decreases with the corresponding ratio of 1.0:0.91:0.80:0.70:0.60:0.50. The decrease in the total heat evolved during polymerization tracks the decrease in concentration of the thiol–ene monomer system, suggesting that the presence of the LC component does not reduce the functional group reactivity significantly. The decrease in rate that does occur is consistent with both a decrease in the concentration of the thiol and ene monomers as well as a contribution from the decrease in light absorbed by the photoinitiator. This confirms that the thiol–ene mixtures in this investigation can be readily cured to give high conversions of crosslinked networks.

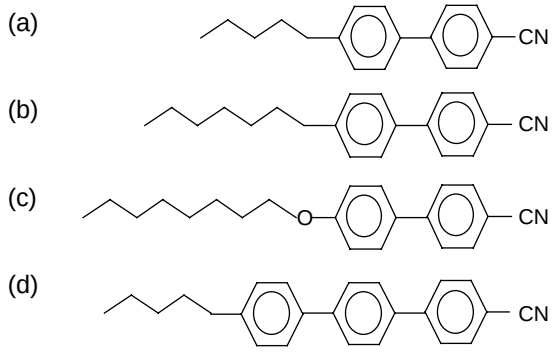

Diagram 2. Chemical structures of the LC mixture of E7, (a) K15 (51 wt%), (b) K21 (25 wt%), (c) M24 (16 wt%), and (d) T15 (8 wt%).

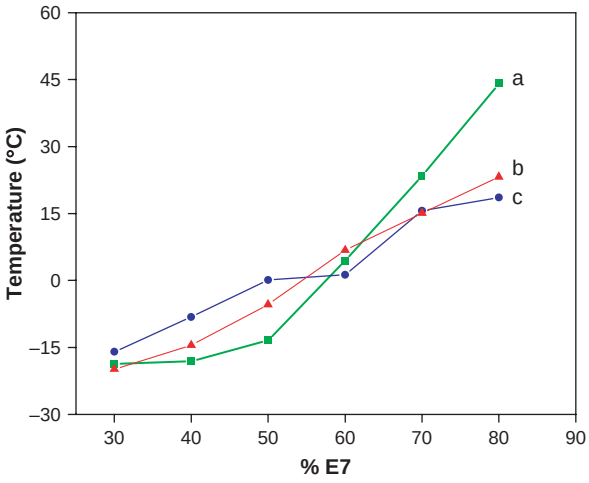

Fig. 1. Phase diagrams of pre-polymerization mixtures of (a) trithiol-triallyloxytriazine, (b) trithiol-pentaerythritol triallyl ether, and (c) trithiol-triallyltriazine trione containing 30–80 wt% E7 obtained with the optical microscopy.

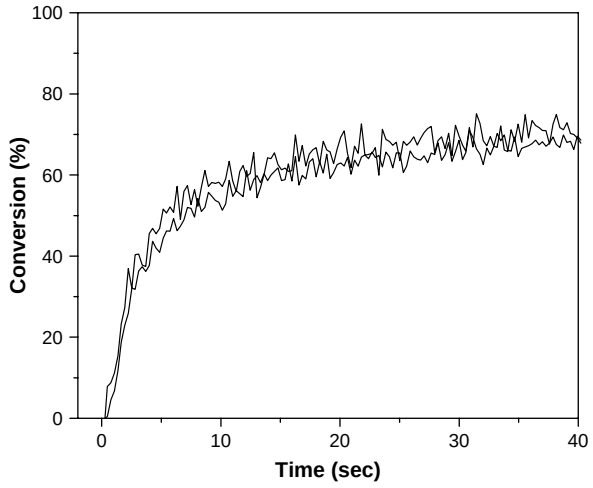

Fig. 3. RTIR thiol-ene conversions of 1:1 molar mixtures of trithiol-triallyltriazine trione in N_2 with 1.0 wt% DMPA (light intensity 1.4 mW/cm^2 at 365 nm, high pressure mercury-xenon lamp source).

3.3. Mechanical/physical properties of photocured thiol–ene networks

DSC temperature scans (10 °C/min scan rate) of thoroughly photocured films (medium pressure mercury lamp) reveal that the pure photocured trithiol-pentaerythritol triallyl ether polymer matrix has a glass transition (T_g) of −12 °C. The T_g decreases from −12 to −23 °C as the LC (E7) weight percentage increases from 0 to 30% (Fig. 5). Unreactive LC small molecules suppress the T_g of the polymer matrix due to a plasticizing effect. The T_g of the LC/polymer matrix reaches a lower limit at 30 wt% LC concentration. A further increase in the LC concentration in the polymer matrix does not change the T_g, i.e. at higher LC concentrations phase separation occurs and a separate LC rich phase forms. DMA analysis of the cured trithiol-pentaerythritol triallyl ether/LC mixture is in agreement with the DSC analysis as shown in Fig. 6. The peak maximum of the tan delta plot decreases with increasing LC concentration in the polymer matrix and reaches a lower limit at 30 wt% LC concentration. Higher concentrations of E7 do not change the mechanical properties of the polymer matrix, which is saturated with LC molecules for samples with greater than 30 wt% E7. Summary plots of thermal transition temperatures for all cured trithiol/triene/E7 mixtures obtained by DSC and DMA (Figs. 7 and 8, respectively) indicate the same tendency, i.e. a decrease in T_g with LC content up to a certain critical LC concentration. We note that the tan delta peak temperatures obtained with DMA for a given sample are always higher than the glass transition temperatures measured with the DSC, consistent with other studies [55]. This results from the faster scanning frequency for DMA versus DSC. The LC/polymer films obviously exhibit a variation in T_g due to the different molecular structure of the ene monomers. Trithiol-triallyltriazine trione polymer matrices have the highest T_gs

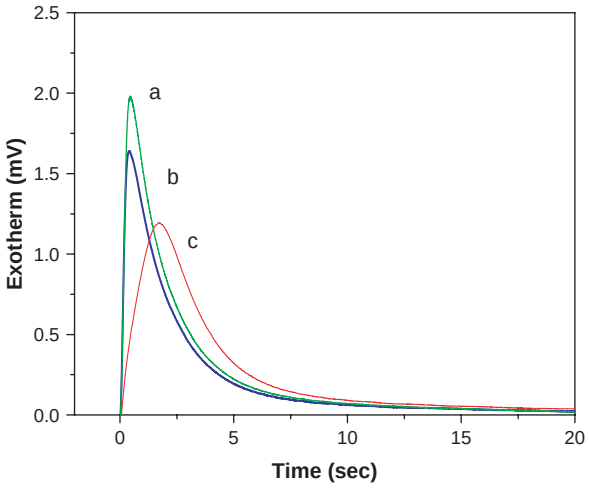

Fig. 2. Polymerization exotherms of (a) trithiol-triallyloxytriazine, (b) trithiol-triallyltriazine trione, and (c) trithiol-pentaerythritol triallyl ether obtained with TFC. Light intensity 1.85 mW/cm^2 at 365 nm (medium pressure mercury light source).

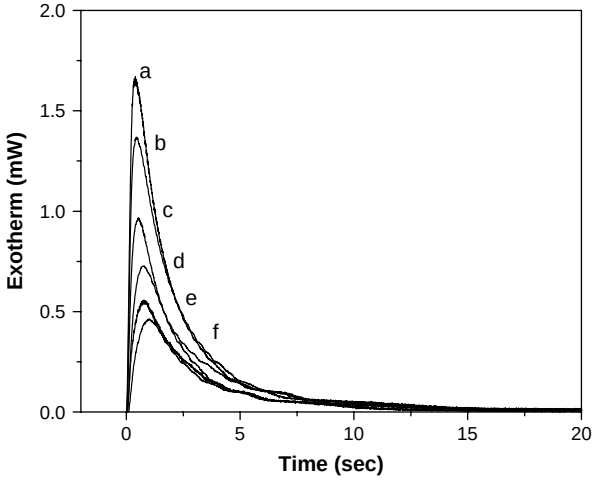

Fig. 4. Polymerization exotherms of trithiol-triallyltriazine trione films (10 μm thickness) with (a) 0 wt%, (b) 10 wt%, (c) 20 wt%, (d) 30 wt%, (e) 40 wt%, (f) 50 wt% LCs obtained with thin-film calorimetry (6.13 mW/cm^2, medium pressure mercury lamp).

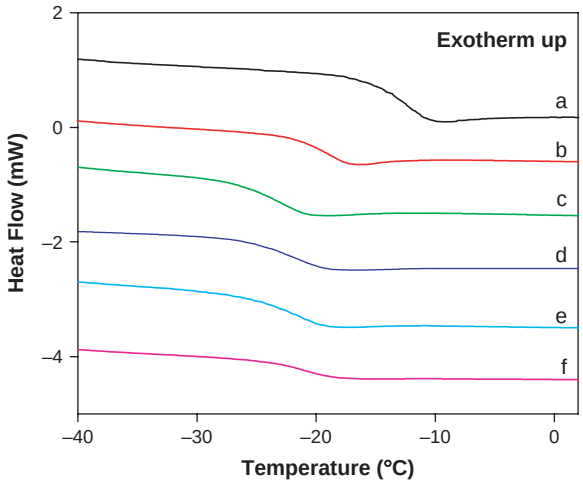

Fig. 5. Thermal transitions of trithiol-pentaerythritol triallyl ether films cured under UV Fusion EPIQ 6000 (D bulb 3.15 W/cm^2 at a line speed of 10 ft/min) with (a) 0 wt% E7, (b) 10 wt% E7, (c) 20 wt% E7, (d) 30 wt% E7, (e) 40 wt E7, and (f) 50 wt% E7 obtained with DSC, scanning rate of 10 °C/min.

due to the rigidity of the ring in the ene monomer (Figs. 7(a) and 8(a)). The rigid ring structure significantly restricts the motion of the polymer matrix, which in turn increases the T_g. Propylene oxide side groups attached to the aromatic ring in triallyloxytriazine provide flexibility to the trithiol-triallyloxytriazine polymer matrix and decrease the T_g by ~20 °C compared to the corresponding trithiol-triallyltriazine trione based films (Figs. 7(b) and 8(b)). The polymer films made with trithiol-pentaerythritol triallyl ether/LC have the lowest glass transition temperatures due to the flexible allyl ether linkages in the polymer backbone (Figs. 7(c) and 8(c)). Finally, we summarize by concluding that the DMA results from this section, which are closer to the frequencies associated with electro-optic switching, suggest that films formed from trithiol-pentaerythritol triallyl ether/LC mixtures are rubbery at room temperature while those fabricated from trithiol-triallyltriazine

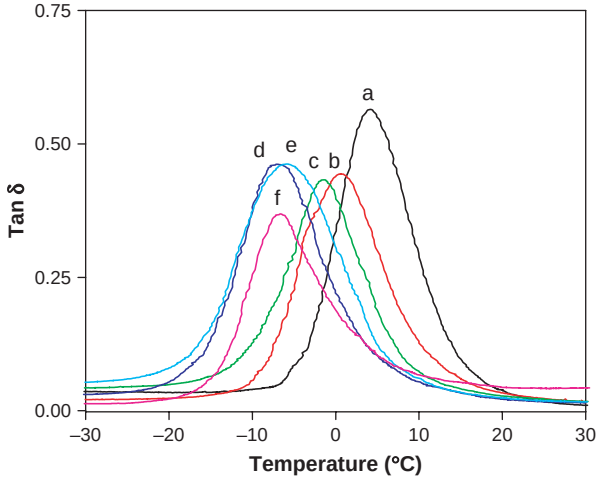

Fig. 6. The tan δ peak maxima of trithiol-pentaerythritol triallyl ether films cured under UV Fusion line EPIQ 6000 (D bulb 3.15 W/cm^2 at a line speed of 10 ft/min) with (a) 0 wt% E7, (b) 10 wt% E7, (c) 20 wt% E7, (d) 30 wt% E7, (e) 40 wt% E7, and (f) 50 wt% E7 obtained with DMA, at a scan rate 3 °C/min.

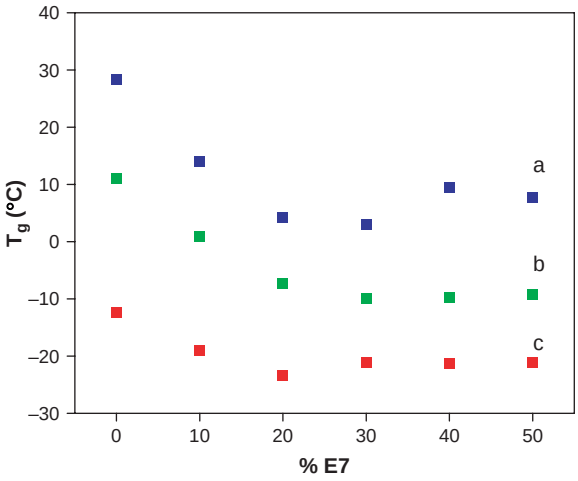

Fig. 7. The summary of glass transition temperatures (T_g) of (a) trithiol-triallyltriazine trione, (b) trithiol-triallyloxytriazine, and (c) trithiol-pentaerythritol triallyl ether obtained with DSC (10 °C/min scanning rate).

trione and trithiol-triallyloxytriazine are glassy for electro-optic switching purposes. This information will be used to interpret the switching results in Section 3.5 and provide a rationale for correlating the physical nature of the thiol–ene matrix with electro-optic switching parameters.

3.4. H-PDLC morphological characterization

Transmission hologram gratings were recorded in the Bragg regime (spacing less than 1.5 μm) by illuminating thiol–ene/LC mixtures with the interference pattern created by the splitting and recombination of the output beam from an argon ion laser (λ = 364 nm). The interference pattern of the split laser beam forms dark and bright regions in the initial monomer/LC mixture. Since the polymerization rate is proportional to the light intensity, the difference in the reaction rate in different regions ensures the periodic phase separation of LC molecules from the emerging polymer

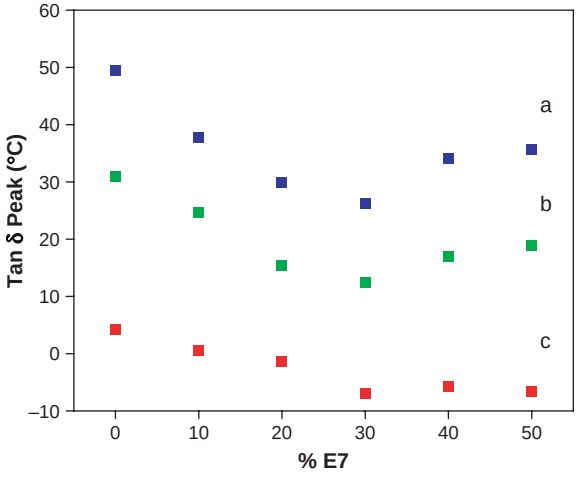

Fig. 8. The summary of the tan δ peak maximums of (a) trithiol-triallyltriazine trione, (b) trithiol-triallyloxytriazine, and (c) trithiol-pentaerythritol triallyl ether obtained with DMA, at frequency 1 Hz.

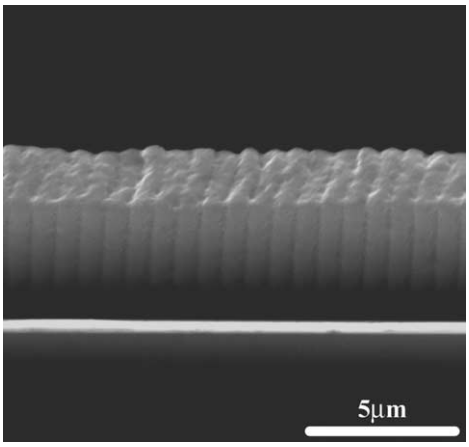

Fig. 9. SEM images of trithiol-triallyloxytriazine with 40 wt% E7 H-PDLC which illustrates the uniformity of the polymer and liquid crystal droplet planes. The scale bar 5 μm.

matrix. According to previous descriptions [28–30] of the behavior of LC molecules in thiol–ene systems, phase separation occurs prior to the gel point, while both LC and monomer/oligomers are in the liquid phases, due to the slow molecular weight built up before gelation. As an example of the type of morphology that can be achieved with the trithiol–ene systems, Fig. 9 shows an SEM image of a H-PDLC formed from trithiol-triallyloxytriazine with 40 wt% E7 that illustrates the uniformity of the alternating liquid crystal droplet and polymer planes. The grating spacing of the sample in Fig. 9 is approximately 1.1 μm with droplet sizes between 0.1 and 0.3 μm in diameter. The SEM image of the other trithiol–ene systems investigated were similar in general structure to the SEM images in Fig. 9: an example of the effect of variation in the LC concentration on the droplet sizes and the number of droplets per unit volume for each thiol–ene combination is illustrated by SEM images for two trithiol-pentaerythritol triallyl ether samples, one with 35 wt% and the other with 50 wt% E7. The droplet planes were more uniform and well-defined for the sample with the lower E7 percentage in that the droplet planes are one droplet wide. At the higher LC concentration, the LC droplet planes are less well defined and the droplets larger (Fig. 10). A similar general trend is observed for the other trithiol–ene/LC systems with increasing LC concentration.

3.5. H-PDLC electro-optic characterization

Analysis of the electro-optic parameters of the H-PDLCs yields insight into the effect of the physical structure of the thiol–ene matrix and LC concentration on the switching voltages and times. Consider first the results for the H-PDLCs obtained from the trithiol-pentaerythritol triallyl ether/E7 mixtures. The voltage required to achieve 90% response, V_{90}, ranges from 6.2 to 5.4 V/μm as the LC percentage in the initial mixture increases from 30 to 50 wt% (Table 1): these switching voltages are relatively low. The decrease in the switching voltage with LC concentration reflects the larger size of the droplets (see Fig. 10 for reference). V_{90} ranges from 11.4 to 6.9 V/μm for the H-PDLCs obtained from the trithiol-triallyltriazine trione/E7 mixtures over the same LC compositional range (Table 2). Similar V_{90} values were obtained for the trithiol-triallyloxytriazine/E7 H-PDLCs (Table 3). Interestingly, SEM analysis of the grating structures and LC droplet sizes revealed a similarity in the morphologies for each of the three base polymeric systems. Therefore, the differences in V_{90} values for the trithiol-pentaerythritol triallyl ether/E7 mixtures compared to both the trithiol-triallyltriazine trione and trithiol-triallyloxytriazine mixtures with E7 are most likely due to the physical structure of the thiol–ene matrix as opposed to spatial aspects (droplet size, shape, and etc.) of the phase separated morphology. In particular, we point out that the glass transitions (maxima in the tan δ plots) that are given in Fig. 8 for the trithiol-pentaerythritol triallyl ether samples with 30–50 wt% LC are well below room temperature where the switching measurements were made. Note that the actual glass transition temperatures that are operative at the rapid switching rates (greater than 1 Hz) will be larger than those inferred from the tan δ plots determined at 1 Hz. The electro-optic results for all of the trithiol-pentaerythritol triallyl ether based H-PDLCs were obtained for samples that are in the

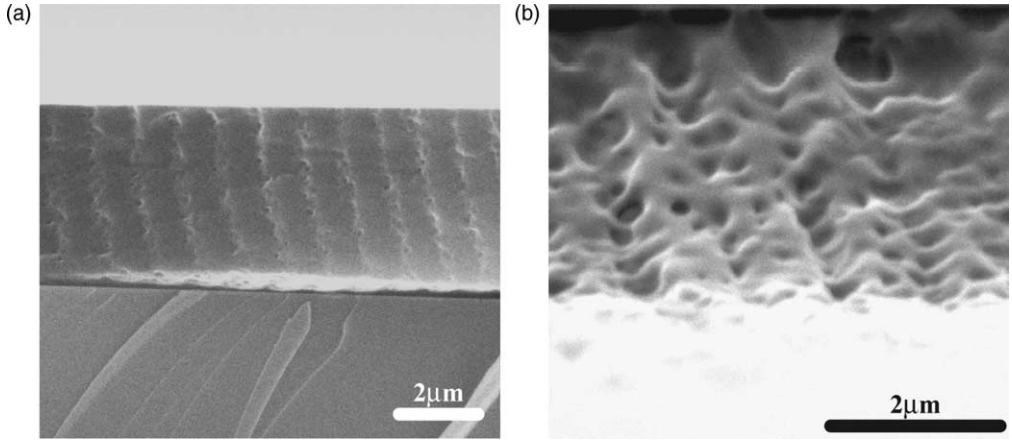

Fig. 10. SEM images of trithiol-pentaerythritol triallylether H-PDLC films with (a) 35 wt% and (b) 50 wt% E7. The scale bar in each image is 2 μm.

Table 1
Summary table of electro-optic responses of trithiol-pentaerythritol triallyl ether H-PDLC films with 30–50 wt% E7

%LC	t_{switch} (ms)	V_{90} (V/μm)
30	1.70	6.2
40	1.40	6.79
50	1.20	5.39

rubbery region as indicated in the summary to Section 3.3. This is not true for the electro-optic results for the trithiol-triallyltriazine trione and trithiol-triallyloxytriazine based H-PDLCs which, at the very rapid switching rates recorded, are most assuredly in the glassy state. Next, we note that the switching times for the H-PDLCs based upon trithiol-pentaerythritol triallyl ether/E7 mixtures were all less than 2.0 ms, whereas the switching time for trithiol-triallyloxytriazine/E7 and mixtures trithiol-triallyltriazine trione/E7 mixtures were substantially greater. Remembering that the electro-optic switching measurements were performed at room temperature, we propose that the much lower glass transition temperatures for the trithiol-pentaerythritol triallyl ether/E7 based H-PDLCs have a distinct effect on causing the lower switching times, as well as the V_{90} values previously discussed. Finally, we mention that longer switching times could also potentially result from modification of the LC composition due to preferential phase separation: however, microscopy results of nematic-to-isotropic transition temperatures indicate that this is not the case.

Although, as stated in the introduction, it was not the objective of the present investigation to fabricate H-PDLCs with optimum diffraction efficiencies, which would require selection of LC components based upon their refractive index properties with respect to the thiol–ene matrix, we nonetheless measured diffraction efficiencies for each system. Accordingly, it is no surprise that the diffraction efficiencies measured were all low (from 2 to 9): see Fig. 11 for an example of a typical diffraction versus time plot where the diffraction efficiency was computed by finding the ratio of the 1st order diffraction intensity to the sum of the 1st order and zero order intensities. The small scale variation of the

Table 2
Summary table of electro-optic responses of trithiol-triallyltriazine trione H-PDLC films with 30–50 wt% E7

%LC	t_{switch} (ms)	V_{90} (V/μm)
30	4.60	11.4
40	4.60	10.3
50	6.70	6.94

Table 3
Summary table of electro-optic responses of trithiol-triallyloxytriazine H-PDLC films with 30–50 wt% E7

%LC	t_{switch} (ms)	V_{90} (V/μm)
30	3.10	12.2
40	1.70	11.3
50	1.80	9.85

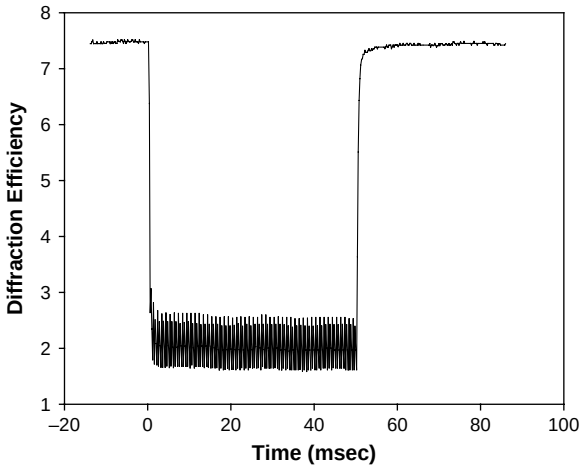

Fig. 11. Applied voltage dependent diffraction efficiency for an H-PDLC film prepared from trithiol-pentaerythritol triallyl ether with 30 wt% E7.

diffraction efficiency in the 0–50 ms time span (i.e. during the application of external applied waveform of 50 ms duration with 1 kHz modulation) is due to collective molecular oscillation about the equilibrium orientation as a result of the applied waveform. We note that in addition to the refractive index matching considerations between the LC droplets and the matrix already mentioned, the diffraction efficiencies were measured at off Bragg angles, which contributes to the low values. For the purposes of this paper, we simply mention that there was no obvious repeatable variation in the diffraction efficiencies measured based upon the thiol–ene structure. Optimization of diffraction efficiencies would require careful choice of the LC mixture and the thiol–ene matrix based upon an extension of the type of investigation conducted herein.

4. Conclusions

A systematic investigation of the effect of thiol–ene structure on the physical, mechanical, and electro-optic properties of H-PDLC photocurable systems has been conducted. The results indicate that the chemical structures of the components comprising the thiol–ene/liquid crystal formulation dictate the physical properties of the resultant films and play a role in the electro-optic performance of fabricated H-PDLCs. In each case, as the liquid crystal content increased for a given matrix type, the switching time decreased due to the presence of larger droplets. In addition, shorter switching times and lower switching voltages were recorded for samples with glass transitions below room temperature. This paper clearly shows that it is important to consider the chemical structures of the thiol and ene components upon which the H-PDLCs are based. There is a direct correlation between the physical state of the polymer matrix (glassy, rubbery) and the electro-optic switching properties of the liquid crystals, with samples that are clearly in the rubbery state and well above their glass transition exhibiting lower switching voltages and faster switching times.

Acknowledgements

This work was supported by AFOSR (DEPSCoR), NSF (DMR-9512506) and the MRSEC Program of the National Science Foundation under Award Number DMR 0213883.

References

[1] Sarkar MD, Gill NL, Whitehead JB, Crawford GP. Macromolecules 2003; 36:630–8.
[2] Bowley CC, Fontecchio AK, Crawford GP. Appl Phys Lett 2000;76(5): 523–5.
[3] Olenik ID, Jazbinsek M, Sousa ME, Fontecchio AK, Crawford GP, Copic M. Phys Rev E 2004;69(5):051703–051710.
[4] Vilfan M, Zalar B, Fontecchio AK, Vilfan M, Escuti MJ, Crawford GP, et al. Phys Rev E 2002;66(2):021710–021719.
[5] Qi J, Desarkar M, Warren GT, Crawford GP. J Appl Phys 2002;91(8): 4795–800.
[6] Bowley CC, Crawford GP, Yuan H. Appl Phys Lett 1999;74(21):3096–8.
[7] Xianyu H, Qi J, Cohn RF, Crawford GP. Opt Lett 2003;28(10):792–4.
[8] Escuti MJ, Qi J, Crawford GP. Opt Lett 2003;28(7):522–4.
[9] Bowley CC, Crawford GP. Appl Phys Lett 2000;76(16):2235–7.
[10] Escuti MJ, Kossyrev P, Crawford GP, Fiske TG, Colegrove J, Silverstein LD. Appl Phys Lett 2000;77(26):4262–4.
[11] Jazbinsek M, Olenik ID, Zgonik M, Fontecchio AK, Crawford GP. J Appl Phys 2001;90(8):3831–7.
[12] Qi J, Sousa MA, Fontecchio AK, Crawford GP. Appl Phys Lett 2003; 82(9):1–3.
[13] White TJ, Guymon CA. Polym Mater Sci Eng 2003;89:452–3.
[14] Shin EY, Jung JA, Kim EH, Kim BK. Polym Int 2005;54:922–5.
[15] Cho YH, Kim BK, Park KS. Polym Int 1999;48:1085–90.
[16] Lucchetta DE, Criante L, Simoni F. Opt Lett 2003;28(9):725–7.
[17] Liu LJ, Zhang B, Jia Y, Xu KS. Opt Commun 2003;218:27–32.
[18] Tanaka K, Kato K, Date M. Jpn J Appl Phys 1999;38:L277–L8.
[19] Date M, Takeuchi Y, Kato K. J Phys D: Appl Phys 1998;31:2225–30.
[20] Date M, Takeuchi Y, Kato K. J Phys D: Appl Phys 1999;32:3164–8.
[21] Woo JY, Park MS, Kim BK, Kim JC, Kang YS. J Macromol Sci, Part B 2004;B43(4):833–43.
[22] Park MS, Kim BK, Kim JC. Polymer 2003;44:1595–602.
[23] Holmes ME, Malcuit MS. Phys Rev E 2002;65(6):066603–066604.
[24] Colvin VL, Larson LG, Harris AL, Schilling ML. J Apply Phys 1997; 81(9):5913–23.
[25] Kyu T, Nwabunma D, Chiu HW. Phys Rev E 2001;63(6): 061802–061808.
[26] Karasawa T, Taketomi Y. Jpn J Appl Phys 1997;36:6388–92.
[27] Bunning TJ, Natarajan LV, Tondiglia VP, Sutherland RL. Ann Rev Mater Sci 2000;30:83–115.
[28] Natarajan LV, Shepherd CK, Brandelik DM, Sutherland RL, Chandra S, Tondiglia VP, et al. Chem Mater 2003;15:2477–84.
[29] Bunning TJ, Natarajan LV, Tondiglia VP, Dougherty G, Sutherland RL. J Polym Sci, Part B 1997;35:2825–33.
[30] Natarajan LV, Tondiglia VP, Sutherland RL, Tomlin D, Bunning TJ. Polym Mater Sci Eng 2003;89:48–9.
[31] Pogue RT, Natarajan RV, Siwecki SA, Tondiglia VP, Sutherland RL, Bunning TJ. Polymer 2000;41:733–41.
[32] Bunning TJ, Natarajan LV, Tondiglia VP, Sutherland RL, Vezie DL, Adams WW. Polymer 1995;36:2699–708.
[33] Bunning TJ, Natarajan LV, Tondiglia VP, Sutherland RL, Vezie DL, Adams WW. Polymer 1996;37(14):3147–50.
[34] Sutherland RL. J Opt Soc Am B 2002;19(12):2995–3003.
[35] Sutherland RL, Natarajan LV, Tondiglia VP, Chandra S, Shepherd CK, Brandelik BM, et al. J Opt Soc Am B 2002;19(12):3004–12.
[36] Sutherland RL, Tondiglia VP, Natarajan LV, Bunning TJ. Appl Phys Lett 2001;79(10):1420–2.
[37] Pogue RT, Sutherland RL, Schmitt MG, Siwecki SA, Tondiglia VP, Bunning TJ. Appl Spectrosc 2000;54(1):12A–228.
[38] Klosterman AM, Pogue RT, Schmitt MG, Natarajan LV, Tondiglia VP, Tomlin D, et al. MRS Proc 1999;559:129–34.
[39] Tanaka K, Kato K, Date M, Sakai S. SID Dig Tech Pap 1995;26:267.
[40] Crawford GP, Fiske TG, Silverstein LD. SID Dig Tech Pap 1996;27:99.
[41] Bunning TJ, Natarajan LV, Sutherland RL, Tondiglia VP. SID Dig Tech Pap 2000;31:121.
[42] Sutherland RL, Natarajan LV, Tondiglia VP, Adams WW. Appl Phys Lett 1994;64(9):1074–6.
[43] Nelson AR, Chen T, Jauniskis L, Domash L. Proc SPIE 1995;2404:182.
[44] Fontecchio AK, Bowley CC, Crawford GP. Proc SPIE 1999;3800:36.
[45] Domash LH, Chen YM, Gozewski C, Haugsjaa P, Oren M. Proc SPIE 1997;3010:214.
[46] Jacobine AF. In: Fouassier JD, Rabek JF, editors. Radiation curing in polymer science and technology 3. London: Elsevier Applied Science; 1993. p. 219 [chapter 7].
[47] Cramer NB, Bowman CN. J Polym Chem A 2001;39(9):3311–9.
[48] Hoyle CE, Lee TY, Roper T. J Poly Sci, Part A 2004;42(5301):5301–38.
[49] Hoyle CH, Hensel RD, Grubb MB. Polym Photochem 1984;4(1):69–80.
[50] Hoyle CH, Hensel RD, Grubb MB. J Polym Sci, Poly Chem Ed 1984; 22(8):1865–73.
[51] Wisnosky YD, Fantazier RM. J Radiat Curing 1981;8(4):20–3.
[52] Pargellis AN. Rev Sci Instrum 1986;57(7):1384–7.
[53] Rajaram CV, Hudson SD, Chein LC. Chem Mater 1996;8(10):2451–60.
[54] Smith GE. Int J Mod Phys B 1993;7(25):4187–213.
[55] Nazarenko S, Haderski A, Hiltner A, Baer E. Polym Eng Sci 1995;35: 1682–7.